Journal of Alloys and Compounds 509 (2011) 147–151

Contents lists available at ScienceDirect

Journal of Alloys and Compounds

journal homepage: www.elsevier.com/locate/jallcom

Structural studies on iron–tellurite glasses prepared by sol–gel method

S. Rada [a,*], A. Dehelean [a,b], M. Stan [b], R. Chelcea [a,b], E. Culea [a]

[a] Department of Physics, Technical University of Cluj-Napoca, Bibliotecii, No. 10, 400020 Cluj-Napoca, Romania
[b] Nat. Inst. for R&D of Isotopic and Molec. Technologies, Cluj-Napoca, Romania

ARTICLE INFO

Article history:
Received 28 June 2010
Received in revised form 31 August 2010
Accepted 1 September 2010
Available online 21 September 2010

Keywords:
Iron–tellurite glasses
FTIR
UV–vis and EPR spectroscopy

ABSTRACT

In this study, we report structural properties of the iron–tellurite glasses obtained using the sol–gel synthesis. The samples were characterized by X-ray diffraction, FTIR, UV–vis and EPR spectroscopy. Our results indicate dominant presence of iron ions in the trivalent state and the existence some Fe^{2+} ions. The analysis of the IR spectra indicates a gradual transformation of iron ions from tetrahedral into octahedral sites when the concentration of $Fe(NO_3)_3$ is increased beyond 0.64 mol%. EPR studies show that the increase of $Fe(NO_3)_3$ content in the host matrix induces the growth of the number of effective *g* values. This can be explained considering that the orbitals of O^{2-} ion with a large spin–orbit interaction constant will interact with the 3d orbital of Fe^{3+} ion bonded to this O^{2-} ion, thus leading to appearance of an orbital angular momentum which contributes to the magnetic moment of Fe^{3+} ion. A strong dipolar interaction, which is more predominant in a glass with higher content of $Fe(NO_3)_3$, causing a localized magnetic field along the site of the Fe^{3+} ions and the increase the effective *g* values.

1. Introduction

The sol–gel process for the preparation of glasses and ceramics has attracted increasing scientific and technological interest [1]. Tellurite materials have been studied for some years due to high refractive index (in the range from 1.85 to 2.2), high non-linear third order optical susceptibility (50 times higher than one of SiO_2 systems), high transmittance from ultraviolet to near infrared, low glass transition temperature and electrical semiconductivity [2–7]. Tellurite materials are also important for high ionic conductivity [8–11]. Due to these properties tellurium glasses are ideal materials for applications in many important fields like telecommunication technology, laser and optical fibre technology, optical device technology [12,13].

Iron ions have a strong bearing on optical, magnetic and electrical properties of glasses [14–16]. A large number of interesting studies are available on the environment of iron ions in various inorganic glass systems (e.g.: silicate, borate, phosphate, germanate, tellurite glasses). These ions exist in different valence states with different coordinations in glass matrices, for example, as Fe^{3+} with both tetrahedral and octahedral and as Fe^{2+} with octahedral environment. Both Fe^{3+} and Fe^{2+} ions are well-known paramagnetic ions. The Fe^{2+} ion has a large magnetic anisotropy due to its strong spin–orbit interaction of the 3d orbital whereas such anisotropy energy of Fe^{3+} ions is small because its orbital angular momentum is zero.

The processing route mainly adopted for producing tellurite glasses is a melting and quenching technique, which is difficult to produce homogeneous multicomponent tellurite glasses due to their relatively high volatility, limited stability and ready contamination by crucibles. Sol–gel process is an attractive alternative to overcome these drawbacks [17].

Sol–gel processing is an attractive method to prepare vitreous materials since the variety of preparative methods and ready availability of a large number of starting materials have provided the feasibility to produce various materials [18].

The conventional hydrolytic sol–gel routes involved two types of chemical reaction. First, the hydroxylation of inorganic or organic-metal precursors is achieved either by varying the pH in an aqueous solvent for inorganic metal salts or by hydrolyzing metal alkoxides in an organic solvent. Second, the condensation of the hydroxyl groups leads to the formation of the oxide network. Eqs. (1)–(4) summarize some of the reactions involved during the hydrolysis-condensation of metal alkoxides [10].

$$(RO)_nM + H_2O \xrightarrow{\text{hydrolysis}} (RO)_{n-1}M\text{–}OH + ROH \quad (1)$$

$$2(RO)_{n-1}M\text{–}OH \xrightarrow[\text{condensation}]{\text{water}} [(RO)_{n-1}M]_2O + H_2O \quad (2)$$

* Corresponding author.
E-mail addresses: Simona.Rada@phys.utcluj.ro, radasimona@yahoo.com (S. Rada).

0925-8388/$ – see front matter © 2010 Elsevier B.V. All rights reserved.
doi:10.1016/j.jallcom.2010.09.011

Table 1
Molar ratios of the starting materials for $Fe(NO_3)_3$–TeO_2 glasses.

Sample	Molar ratios					
	$Te(OEt)_4$	$Fe(NO_3)_3{\cdot}9H_2O$	EtOH	CH_3COOH	H_2O	$(CH_2OH)_2$
1	1	0.16	19.4	35.93	–	–
2	1	0.32	19.4	35.93	–	–
3	1	0.64	19.4	35.93	–	–
4	1	0.80	19.4	35.93	–	–
5	1	0.80	19.4	39.93	6.94	20

or

$$(RO)_{n-1}M\text{–}OH + (RO)_nM \xrightarrow[\text{condensation}]{\text{alcohol}} [(RO)_{n-1}M]_2O + ROH \quad (3)$$

$$M\text{–}OR + RO\text{–}M \rightarrow M\text{–}O\text{–}M + ROR \quad (4)$$

The present study is aimed to investigate the structural properties of some iron–tellurite glasses synthesized by sol–gel method. The structural modifications were analyzed by investigations of FTIR, UV–vis and EPR spectroscopy.

2. Experimental details

A series of iron–tellurite vitreous systems were prepared by sol–gel synthesis using two preparation methods. For the first method, tellurium (IV) ethoxide (85%) and stoichiometric quantities of iron (III) nitrate, ($Fe(NO_3)_3{\cdot}9H_2O$ (98%, metals basis), absolute ethanol and glacial acetic acid, were employed for sol–gel synthesis. Tellurium (IV) ethoxide was dissolved in ethanol, followed by addition of iron (III) nitrate and glacial acetic acid under continuous stirring until the reaction mixture became homogeneous. Then, the reaction mixture was stirred for 45 min at 333 K in atmospheric conditions. After filtration, the wet gel obtained was dried in the oven for 24 h at 353 K, and was ground to give fine powder.

In the second method, tellurium (IV) ethoxide (85%) was diluted with ethylene glycol, followed by addition of iron (III) nitrate, ($Fe(NO_3)_3{\cdot}9H_2O$, 98%, metals basis) dissolved in ethanol and glacial acetic acid. In this case, the reaction mixture was stirred for 1 h at 333 K in atmospheric conditions. The solution was settled down overnight, followed by addition of deionized water, and then, continuous stirring for 1 more hour at 333 K. Likewise, after filtration, the wet gel formed was dried in the oven for 24 h at 338 K, and was ground to give fine powder. Table 1 shows the molar ratios of the starting materials for preparation of iron doped-TeO_2 vitreous systems.

Tellurite systems prepared by a controlled sol–gel reaction were analyzed by means of X-ray diffraction using a XRD-6000 Shimadzu Diffractometer, with a monochromator of graphite for Cu-Kα radiation (λ = 1.54 Å) at room temperature.

The infrared absorption spectra of the glasses were recorded using a JASCO FTIR 6200 spectrometer in the range of 350–1500 cm^{-1}. The measurements were performed using the KBr pellet technique. The spectra were carried out with a standard resolution of 2 cm^{-1}.

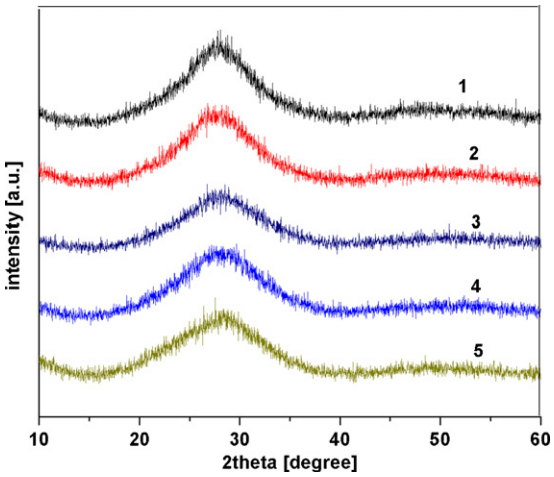

Fig. 1. X-ray diffraction patterns for iron–tellurite glass samples.

UV–vis absorption spectra of the powdered glass samples were recorded at room temperature in the range 250–900 nm using a Perkin–Elmer Lambda 45 UV/vis spectrometer equipped with an integrating sphere. These measurements were made on glass powder dispersed in KBr pellets.

EPR measurements were performed at room temperature using ADANI Portable EPR PS 8400-type spectrometer, in X frequency band (9.2 GHz) and a field modulation of 100 kHz. The microwave power used was 5 mW.

3. Results and discussion

3.1. FTIR spectroscopy

XRD analysis of the structure of tellurite systems obtained showed no distinguishing peaks, which indicates that systems were amorphous (Fig. 1).

A simple inspection of the spectral features presented in Fig. 2a shows that because the majority of the bands are large and asymmetric, presenting also some shoulders, a deconvolution of the experimental spectra was necessary.

The deconvoluted IR spectra for the iron–tellurite glasses are shown in Fig. 2a and the peak assignments are given in Table 2. This deconvoluted allowed us a better identification of all bands that appear in the FTIR spectra in order to realize their assignment. The deconvoluted procedure was made by using the Spectra Manager program [19] and a Gaussian type function. The proportion of the particular structures corresponding to different vibration modes was calculated from the areas of fitter Gaussian bands divided to the total areas of these bands. Each component band is related to some type of vibration in specific structural groups. The concentration of the structural group was considered to be proportional

Table 2
Deconvolution parameters (the band centers C and the relative area A) and the bands assignments for the iron–tellurite glasses.

Sample 1		Sample 2		Sample 3		Sample 4		Sample 5		Assignments
A	C	A	C	A	C	A	C	A	C	
2.68	418	11.50	421	7.12	418	3.09	405	7.79	386	Bending vibrations of Te–O–Te or O–Te–O linkages
3.96	521	7.35	531	15.61	529	8.33	503	6.72	495	Fe–O bonds in [FeO_4] units
3.32	618	3.99	631	4.68	692	3.19	662	6.17	628	Te–O bonds in [TeO4] units
2.82	757	2.44	722	5.09	758	5.05	774	4.57	772	Te–O bonds in [TeO_3] units
3.31	1078	2.4	1076	2.19	1079	1.31	1049	1.87	1070	ethyl group in $Te(OEt)_4$
1.6	1390	1.39	1386	0.57	1386	0.75	1384	0.46	1390	stretching vibrations of NO_3^- group

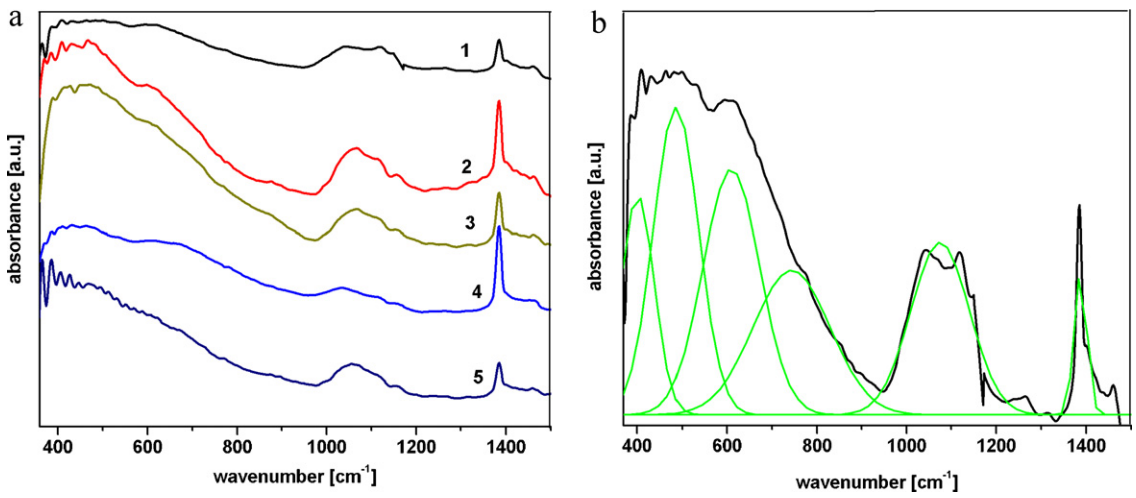

Fig. 2. (a) FTIR spectra of iron–tellurite glass samples obtained by sol–gel method and (b) deconvoluted FTIR spectrum of the sample 1.

to the relative area of its component band [20,21]. The deconvoluted parameters, the band centers, *C* and the relative area, *A* as well as the bands assignment for the studied glass are given in Table 2.

The examination of the FTIR spectra shows that the $Fe(NO_3)_3$ content modifies the characteristic IR bands as follows:

(i) The bands located around 460 cm^{-1}, in the range of 610–680 cm^{-1} and 720–780 cm^{-1} are assigned the bending mode of Te–O–Te or O–Te–O linkages, the stretching mode [TeO_4] trigonal pyramidal with bridging oxygen and the stretching mode of [TeO_3] trigonal pyramidal with non-bridging oxygen, respectively [14–16,22,23]. By increasing $Fe(NO_3)_3$ content up to 0.64 (ration molar) increases the number of [TeO_4] and [TeO_3] structural units. The increasing trends in the intensity of these bands can be due to the formation of bridging bond of Te–O–Te and O–Te–O linkages.

(ii) The bands situated in the 470–600 cm^{-1} range may be ascribed to vibration of the Fe–O bond in the [FeO_6] and [FeO_4] structural units [24]. Iron in the oxidation state +3 is reported to occur predominant in fourfold coordination, as $[FeO_4]^{-1}$. These tetrahedral geometries have a negative charge and hence need cations for compensation of electrical charges. Accordingly, it is possible a better stabilization of Fe^{3+} from $[FeO_4]^{-1}$ tetrahedral units through compensation of electrical charges with Te^{4+} and H^+ ions. The Te^{4+} ions can be derived from $Te(OEt)_4$ starting precursor. These modifications may be attributed to the presence of [TeO_4] and [FeO_4] structural units which will improve the environment of amorphous character.

(iii) The band centered at about 1057 cm^{-1} can be due to the ethyl group in $Te(OEt)_4$ [25]. From Table 1 can be observed that the number of ethyl group in $Te(OEt)_4$ decreases by increasing of $Fe(NO_3)_3$ content up to 0.80. Accordingly, the accumulation of oxygen can be supported into the glass network by the formation of [FeO_6] structural units.

(iv) The absorption band situated at about 1380 cm^{-1} belongs to the asymmetric stretching vibrations of NO_3^- group. This band attains maximum value for sample 1.

In brief, the analysis of the IR spectra indicates a gradual transformation of iron ions from tetrahedral into octahedral sites when the concentration of $Fe(NO_3)_3$ is increased up to 0.8.

3.2. UV–vis spectroscopy

Among all the transition metal ions, Fe^{3+} ion (with d^5 configuration) is of special interest because it is the only configuration for which there is no spin allowed transitions possible and only weak bands may occur corresponding to spin-forbidden transitions. The UV–vis absorption spectra of glass samples are shown in Fig. 3. The examinations of these spectra show that the characteristic UV–vis bands are modified namely:

(i) The bands located in the 300–450 nm region are due to the presence of the Fe^{3+} ions. These bands can be due to the d–d transitions of the Fe^{3+} ions [26–29]. The d–d transitions of the Fe^{3+} ions decrease by increasing of $Fe(NO_3)_3$ content. For sample 1 and 3 some modifications of the bands appear in this region. Then, the apparition of new bands located in the 260–325 nm region is correlated to the possible distortions of symmetry of the iron species. The bands located in the 250–277 nm region are due to a strong oxygen–iron charge transfer derived to the Fe^{2+} and Fe^{3+} ions. The increase in the intensity of the IR band located at about 689 cm^{-1} shows the vibrations of the Fe^{2+}–O–Fe^{3+} linkages [26].

(ii) For samples 1 and 3, three absorption bands located at about 540, 583 and 785 nm are identified due to transitions of the Fe^{3+} ions coordinated with oxygen atoms [26–29]. Based on selec-

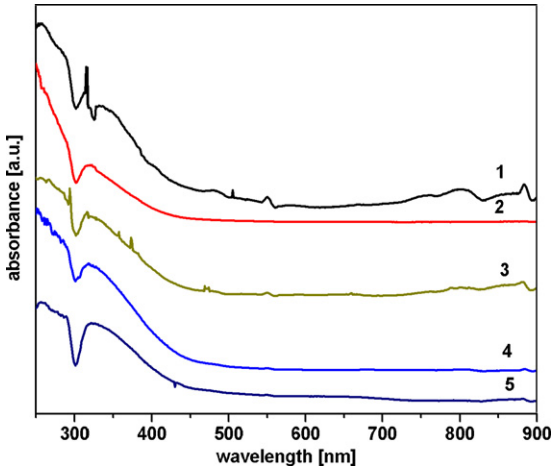

Fig. 3. UV–vis absorption spectra of iron–tellurite glasses in function of $Fe(NO_3)_3$ content.

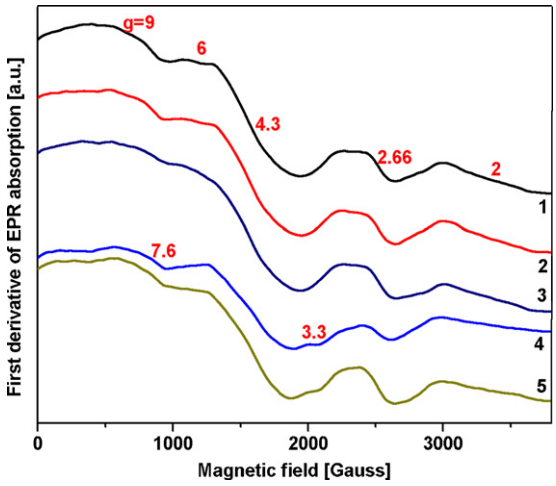

Fig. 4. EPR spectra of iron–tellurite glass samples.

tion rules and ligand field calculations, the first band is due to $[FeO_4]$ structural units while the last bands are identified due to the $[FeO_6]$ structural units. By increasing of $Fe(NO_3)_3$ content, the decrease in the intensity of these peaks show a decrease of the ratio of Fe^{3+} concentrations situated in tetrahedral and hexagonal coordination sites. The four-fold coordination of Fe^{3+} is observed to be more common than the six-fold coordination in many of the glasses [19]. Both these Fe^{3+} sites can be considered as substitutional and subjected to strong interaction between its external orbitals and the p-orbitals of the neighbouring oxygens [27].

(iii) A very sharp absorption band is observed at about 320 nm only for sample 1. This can be explained by presence of a higher number of d–d transitions of the Fe^{3+} ions in this sample. Accordingly, if the $Fe(NO_3)_3$ concentration is low, the Fe^{3+} ions must be considered to behave as modifier and some $[FeO_4] \leftrightarrow [FeO_6]$ interconversion processes were produced.

(iv) Fe^{2+} ions produce a band due to oxygen–iron charge transfer in the ultraviolet [29]. Spin-forbidden bands are also expected in the 450–550 nm domain. Then, Fe^{2+} ions yield absorption bands due to d–d transitions in the near infrared region and can be attributed to a range of distorted octahedral sites. Accordingly, the energy diagram of the $3d^6$ configuration (Fe^{2+}) indicates that its spectrum will consist essentially of a single band in the infrared region as well as a number of very weak spin-forbidden bands in the visible and ultraviolet regions. For samples 1 and 3, the intensity of the bands situated in the infrared region shows that some Fe^{3+} ions were converted to Fe^{2+} ions.

3.3. EPR spectroscopy

Fig. 4 shows EPR spectra of glass samples. These spectra present seven signals at $g \approx 9$, 7.6, 6, 4.3, 3.3, 2.66 and 2. The Fe^{3+} ions can exist in glasses either in the substitutional sites or in the interstitial positions. The resonance signals at $g \approx 4.3$ and 2 were discussed by many investigators [30–34]. They suggested that the value of g in glasses containing Fe^{3+} ions is related to the coordination number. The absorption at $g \approx 4.3$ and 2 arise from Fe^{3+} ions in tetrahedral and octahedral coordination, respectively. The Fe^{2+} ions are not involved in EPR absorption but their interaction with Fe^{3+} may influence the characteristics of the EPR absorption lines. The UV–vis spectrum supports the simultaneous presence of both Fe^{3+} and Fe^{2+}. In the present work, the increase of $Fe(NO_3)_3$ content does strongly modify the characteristic bands of the EPR spectra and can be characterized as follows:

(i) The resonance line located at about $g \approx 4.3$ decreases by increasing of $Fe(NO_3)_3$ content. This signal located at about $g \approx 4.3$ is preferred to in the literature as due to the tetrahedral Fe^{3+} ions in the substitutional site under a rhombic distortion due to the presence of compensating cations in its neighbourhood. The pairs of exchange coupled Fe^{3+} ions can arise from interstitial Fe^{3+} ions after heat treatment which causes a resonance with g-factor around 2. The two signals can be independent of each other, because the amount of interstitial Fe^{3+} ions can vary from sample to sample, depending on the manufacturing process.

(ii) The $g \approx 2$ feature is assigned to a ferromagnetic resonance of the ferromagnetic or ferrimagnetic single domains encounter in glasses [35–37]. Another interpretation about the origin of the signal around $g \approx 2$ is related to the oxygen hole centers that should arise with electron centers. The gradual growing of the signal situated at $g \approx 2$ with the increase in the concentration of $Fe(NO_3)_3$ indicates the formation of Fe^{3+}–O–Fe^{3+} spin pair or clusters of Fe^{3+} ions in glass network.

(iii) The existence of the resonance signals at $g \approx 4.2$ and 7.6 have been attributed to Fe^{3+} ions in rhombic and axial symmetry sites, respectively, whereas the resonance signal at $g \approx 2$ resonance is due Fe^{3+} ions coupled by exchange interactions.

(iv) The signals located at about $g \approx 2.66$ and 3.3 are due to pairs of exchange coupled Fe^{3+} ions. The EPR spectrum reveals presence of the broad band at $g \approx 2.66$. This rarely reported resonance band originates from ferromagnetic couplings of nearby iron cations. The details of the signals located at $g \approx 2.66$ and 3.3 indicate that these signals were chosen for $Fe(NO_3)_3$ content evaluation.

(v) An effective g value of $g \approx 9.7$ was also reported for Fe^{3+} ions in glasses [37,38]. The $g \approx 6$ resonance line is characteristic for isolated Fe^{3+} ions situated from axially distorted sites. For samples 4 and 5, the intensity of the signal situated at about $g \approx 4.3$ increases and a new resonance line located at about $g \approx 3.3$ appears. This can be explained considering that the orbitals of O^{2-} ion with a large spin–orbit interaction constant interact with the 3d orbital of Fe^{3+} ion bonded to this O^{2-} ion, thus leading to the appearance of the orbital angular momentum which contributes to the magnetic moment of Fe^{3+} ion. The strong dipolar interaction, which is more predominant in the glass with the content of $Fe(NO_3)_3$, causes a localized magnetic field at the site of Fe^{3+} ion and increases the effective g value as observed [39,40].

These g values indicate that the paramagnetic ion is in trivalent state and is in distorted octahedral site symmetry. This independence of g values with composition of glass allows us to conclude that the symmetry around the paramagnetic Fe^{3+} ions is independent of concentration of $Fe(NO_3)_3$ present in the samples. Then, increase of $Fe(NO_3)_3$ content implies the appearance of the orbital angular momentum which contributes to magnetic moment of the Fe^{3+} ion and the number of effective g values increases.

4. Conclusions

X ray diffraction, FTIR, UV–vis and EPR spectroscopy studies have been utilized in order to study structural changes produced by the variation of $Fe(NO_3)_3$ content in binary iron–tellurite glasses obtained using the sol–gel method. Our results show that the iron ions located in the glassy matrix are largely in the form of Fe^{3+} ions. The analysis of the IR spectra indicates a gradual transformation of the iron ions from tetrahedral into octahedral sites when

the concentration of $Fe(NO_3)_3$ is increased up to 0.8. The increase of $Fe(NO_3)_3$ content in the host matrix induces the growth of the number of effective *g* values. This can be explained considering that the orbitals of O^{2-} ion with a large spin–orbit interaction constant will interact with the 3d orbital of Fe^{3+} ion bonded to this O^{2-} ion, thus leading to the appearance of a orbital angular momentum which contributes to the magnetic moment of Fe^{3+} ion.

Acknowledgment

The financial support of the Ministry of Education and Research of Romania-National University Research Council (CNMP, Parteneriate, contract number 71099/2007) is gratefully acknowledged by the authors.

References

[1] S. Mathew, P.R. Rejikumar, J. Yohannan, K.T. Mathew, N.V. Unnikrishnan, J. Alloys Compd. 462 (2008) 456.
[2] A. Chagraoui, A. Tairi, K. Ajebli, H. Bensaid, A. Moussaoui, J. Alloys Compd. 495 (2010) 67.
[3] S. Zhao, X. Wang, D. Fang, S. Xu, L. Hu, J. Alloys Compd. 424 (2006) 243.
[4] H. Chen, Y.H. Liu, Y.F. Zhou, Z.H. Jiang, J. Alloys Compd. 397 (2005) 286.
[5] C. Zhao, G.F. Yang, Q.Y. Zhang, Z.H. Jiang, J. Alloys Compd. 461 (1–2) (2008) 617.
[6] A. Ghosh, Philos. Mag. B 61 (1990) 87.
[7] A. Ghosh, J. Phys. Condens. Matter 1 (1989) 7819.
[8] D. Dutta, A. Ghosh, Phys. Rev. B 72 (2005) 024201.
[9] A. Ghosh, A. Pan, Phys. Rev. Lett. 84 (2000) 2188.
[10] A. Pan, A. Ghosh, Phys. Rev. B 59 (1999) 899.
[11] A. Pan, A. Ghosh, Phys. Rev. B 62 (2000) 3190.
[12] A. Clare, Key Eng. Mater. 94–95 (1994) 161.
[13] S. Zhao, X. Wang, D. Fang, S. Xu, L. Hu, J. Alloys Compd. 424 (1–2) (2006) 243.
[14] S. Mandal, A. Ghosh, J. Phys. Condens. Matter 8 (1996) 829.
[15] A. Pan, A. Ghosh, J. Mater. Res. 17 (2002) 1941.
[16] A. Ghosh, J. Appl. Phys. 66 (1989) 2425.
[17] L. Weng, S. Hodgson, X. Bao, K. Sagoe-Crentsil, Mater. Sci. Eng. B 107 (2004) 89.
[18] L.G. Hubert-Pfalzgraf, New J. Chem. 11 (1987) 663.
[19] Microcal (TM) Origin, Version 6.0, Microcal Software, Inc., Northampton, MA 01060, USA.
[20] P. Pascuta, L. Pop, S. Rada, M. Bosca, E. Culea, J. Mater. Sci. Mater. Electron. 19 (5) (2008) 424.
[21] S. Rada, M. Culea, E. Culea, J. Phys. Chem. A 112 (44) (2008) 11251.
[22] S. Rada, M. Culea, E. Culea, J. Non-Cryst. Solids 354 (52–54) (2008) 5491.
[23] S. Rada, M. Rada, E. Culea, Spectrochim. Acta A 75 (2010) 846.
[24] S. Rada, M. Culea, M. Rada, E. Culea, J. Alloys Compd. 490 (2010) 270.
[25] S. Rada, E. Culea, M. Culea, J. Mater. Sci. 43 (2008) 6480.
[26] G.D. Khattak, N. Tabet, L.E. Wenger, Phys. Rev. B 72 (2005) 104202.
[27] R.J.P. Corriu, D. Leclercq, P. Lefevre, P.H. Mutin, A. Vioux, J. Mater. Chem. 6 (1992) 673.
[28] A. Montenero, M. Friggeri, D.C. Giori, N. Belkhiria, L.D. Pye, J. Non-Cryst. Solids 84 (1986) 45.
[29] C.R. Kurkjian, J. Non-Cryst. Solids 3 (1970) 157.
[30] J.W. Park, H. Chen, Phys. Chem. Glasses 23 (1982) 107.
[31] S. Creux, Proc. Fund. Glass Sci. Technol. (1997) 41.
[32] J. Wang, W.B. White, J.H. Adair, J. Am. Ceram. Soc. 88 (2005) 3449.
[33] T. Castner, G.S. Newell Jr., W.C. Holton, C.P. Slichter, J. Chem. Phys. 32 (1960) 668.
[34] D.L. Griscom, J. Non-Cryst. Solids 40 (1980) 211.
[35] D.L. Griscom, C.I. Merzbacher, R.A. Weeks, R.A. Zuhr, J. Non-Cryst. Solids 258 (1999) 34.
[36] R. Debnath, J. Mater. Res. 16 (1) (2001) 127.
[37] I. Ardelean, M. Peteanu, S. Filip, V. Simon, G. Gyorffy, Solid State Commun. 102 (1997) 341.
[38] R.V. Anavekar, N. Devaraj, K.P. Ramesh, J. Ramakrishna, Phys. Chem. Glasses 33 (1992) 116.
[39] T. Komatsu, N. Soga, M. Kunugi, J. Appl. Phys. 50 (1979) 6469.
[40] G. Nagarjuna, N. Venkatramaiah, P.V.V. Satyanarayana, N. Veeraiah, J. Alloys Compd. 468 (2009) 466.